Journal of Environment and Sustainable Mining Vol.1 No.4 (2025) 59-71

Journal of Environment and Sustainable Mining

The Impact of Nano-Microbubbles on Zinc Oxide Ore Flotation Performance

Mohammad Omidifar[1*] , **Sied Ziaedin Shafaei Tonkaboni**[1]

[1] Faculty of Mining Engineering, University of Tehran, Tehran, Iran.

ARTICLE INFO

Article type:
Research Article

Article history:
Received: 2025-10-10
Received in revised form: 2025-11-29
Accepted: 2025-12-22
Available online: 2025-12-29

Keywords:
Sodium sulfide,
Armac C,
Particle size, PAX,
DOE

ABSTRACT

The major challenge in zinc oxide ore flotation is the excessive production of fines during comminution, which leads to increased reagent consumption or the loss of zinc minerals. One of the most effective methods for enhancing recovery is the use of nano-microbubbles in the flotation. In this study, the effect of using nano-microbubbles in the flotation of a zinc oxide ore sample with a Zn content of 15.67% was studied to eliminate the desliming stage. A software-based statistical design of experiments (DOE) was applied to design and statistically analyze the results. The parameters were labeled as: using nano-microbubbles water (A), sodium sulfide concentration as a sulfidant (B), Armac C concentration as a collector (C), and particle size (D). Zinc concentrate recovery was evaluated as the response in the design. Analysis of the results showed that the influence of parameters and their interactions on the response followed the order: B>D>C>BD>BC>CD>A>BCD. Maximum recovery was achieved in the presence of nano-microbubbles, sodium sulfide concentration of 4000 g/t, Armac C concentration of 1000 g/t, and the d80 of the feed particles at 92 µm. Under these conditions, a concentrate with Zn grade of 25.89% and 88.81% recovery was obtained, and in the absence of both nano-microbubbles and PAX as a promoter, the concentrate grade and recovery were 27.31% and 81.74%, respectively. The results showed that using PAX (200 g/t) led to a lower recovery increase (~1%) compared to using nano-microbubbles (~7%).

Cite this article: Naseri, M. , Baqaeifar, M. , Hajilou, M. , Mehdilo, A. and Irannajad, M. (2025). Acid leaching of manganese oxide with hydrochloric acid and willow bark using design expert method. *Journal of Environment and Sustainable Mining*, 1(4), 59-71.
https//doi.org/ 10.22111/jesm.2025.52010.1025

Publisher: University of Sistan and Baluchestan.
DOI: https//doi.org/ 10.22111/jesm.2025.52010.1025

* Corresponding author: **Mohammad Omidifar**
E-mail address: mohammadomidifar95@gmail.com

1. Introduction

Various methods exist to overcome the limitations of flotation caused by the presence of fine particles in the flotation feed. These methods are primarily based on increasing particle size through selective aggregation (including selective agglomeration and flocculation), reducing bubble size (using nano-microbubbles), or employing specialized flotation cells. The low flotation rate of fine particles is mainly due to the low probability of collision between these particles and air bubbles. Previous studies showed that reducing the size of air bubbles can enhance the flotation of fine particles. However, using only small bubbles in the absence of larger bubbles can increase flotation time due to the lower rising velocity and carrying capacity, necessitating the use of taller flotation cells. Therefore, the improvement in flotation is largely attributed to the synergy between normal-sized bubbles and fine bubbles [1]. In addition, the use of small bubbles increases the entrainment of particles, which occurs due to the higher recovery of water. Consequently, it can be concluded that the grade of the product decreases as a result of the entrainment of gangue particles into the concentrate [2].

Flotation of fine particles (<10-20 μm) presents significant challenges due to their low inertia, poor collision efficiency with bubbles, and high surface area, which can lead to excessive reagent consumption and mechanical entrainment [1, 2]. Addressing these issues is crucial for improving overall recovery and concentrate grade. Rezai (2017) demonstrated the effectiveness of nanobubbles in enhancing the flotation of fine phosphate ore particles, highlighting their ability to overcome challenges associated with fine particle recovery [3]. Furthermore, a comprehensive review by Ma et al. (2022) on the characterization and enhancement mechanisms of surface nanobubbles for fine-particle flotation underscored the key role of their unique properties in addressing these challenges [4].

Nanobubbles are extremely small gas cavities in an aqueous solution, with sizes smaller than 1 □m, and they have a lifespan ranging from several days to weeks. Since the work of adhesion between a solid particle and water is always less than the work of adhesion of water, nano-microbubbles selectively accumulate on the surface of hydrophobic particles. Additionally, the work of adhesion decreases with increasing hydrophobicity of the solid particle surface [5]. Nano-microbubbles create a capillary bridge between the surfaces of hydrophobic solid particles, causing these particles to adhere to each other [6]. It has also been established that the flotation rate is strongly influenced by bubble diameter, such that when the bubble diameter decreases from 665 □m to 75 □m, the flotation rate increases by up to 100 times. Thus, it is clear that reducing bubble diameter can lead to enhanced flotation of fine particles [7]. Nazari et al. (2022) concluded that the presence of nano-microbubbles increased the lithium-ion batteries-graphite (LIBG) flotation recovery and its kinetic rate by 15% and 33%, respectively [8]. In addition, one of the influential parameters on the quality of the concentrate and the achievable recovery in the flotation process is froth stability. Due to the presence of an electrical repulsion between the surfaces of nanobubbles, which prevents their coalescence and growth, the presence of nanobubbles significantly impacts froth stability [9]. In a study on copper sulfide flotation in 2024, the presence of nano-microbubbles was found to reduce collector and frother consumption by 50% and 66.6%, respectively [10]. Recent work by Rosa and Rubio (2018) elucidated the intricate interactions between nanobubbles and mineral particles, explaining how nanobubbles significantly improve particle-bubble adhesion and lead to higher flotation efficiency, particularly for fine particles [11]. Moreover, a review by Kyzas et al. (2021) showcased the versatile applications of nanobubble technology, noting their unique properties—such as high specific surface area and prolonged stability—which are particularly advantageous for resource recovery processes like flotation [12]. Nazari et al. (2022) provided a comprehensive review on recent developments in the generation, detection, and application of nanobubbles in flotation. They highlighted advancements in understanding nanobubble behavior and their expanding role in improving mineral recovery processes [13]. Wang et al. (2022) investigated nanobubble-enhanced flotation of ultrafine molybdenite, elucidating the associated mechanisms. Their findings suggested that nanobubbles significantly improve the flotation of ultrafine particles by increasing effective collision probability and promoting strong particle-bubble attachment [14].

Zinjenab et al. (2023) studied the interaction between nano-microbubbles and feed particle size in the flotation of lead and zinc sulfide minerals. Their research revealed that the synergistic effect of optimized feed size and nano-microbubbles significantly enhances flotation performance, particularly for finer particles [15]. Numerous factors influence the size of nano-microbubbles produced, including the method of nano-microbubble generation, the type of frother, frother concentration, gas solubility, solution temperature, gas type, solution pH, and the hydrophobicity of particles [16, 17, 18]. If the generated nanobubbles possess high surface charge density or zeta potential, they will remain stable [18].

One of the major challenges in zinc oxide ores processing is the generation of fines during comminution, which are often separated by hydro-cyclones, leading to the loss of valuable material. One of the methods employed in the flotation of fines is the use of nano-microbubbles alongside conventional bubbles, which is an effective approach for increasing particle recovery. These bubbles enhance the hydrophobicity of particles (in fact, nano-microbubbles are referred to as promoters) to increase the probability of particle-bubble attachment, thereby improving the efficiency of particle collisions. It has also been demonstrated that nano-microbubbles can expand the size range of particles in flotation. Consequently, this study aims to compare the performance of flotation in the presence and absence of nano-microbubbles, without desliming stage, to evaluate the impact of these bubbles on zinc oxide ore flotation.

2. Sample characterization

The sample studied in this research was provided by the Iran Lead and Zinc Plant located in the industrial town of Zanjan Province, Iran. Qualitative and quantitative analysis methods were carried out for the characterization of the sample. X-ray diffraction (XRD) was used for mineral identification, and X-ray fluorescence (XRF) was used to determine the content of various elements or chemical compounds. Additionally, thin and polished sections were used for microscopic mineralogical studies and the determination of the degree of liberation of valuable minerals in the sample.

2.1. Mineralogy

According to the XRD analysis results presented in Table 1, the minerals present in the sample, in order of abundance, include: calcite, smithsonite, quartz, hemimorphite, dolomite, clinochlore, and phlogopite. Therefore, the studied sample is a zinc oxide ore, where smithsonite and hemimorphite are the valuable and economically significant zinc minerals, while the other minerals are considered gangue.

Table 1. Minerals identified in the studied sample using XRD analysis.

Phase	Formula	Semi-quantitative percentage
Calcite	$CaCO_3$	36.2
Smithsonite	$ZnCO_3$	20.7
Quartz	SiO_2	15.9
Hemimorphite	$Zn_4Si_2O_7(OH)_2.H_2O$	9.1
Dolomite	$CaMg(CO_3)_2$	9.1
Clinochlore	$(Mg,Al,Fe)_6(Si,Al)_4O_{10}(OH)_8$	4.5
Phlogopite	$KMg_3AlSi_3O_{10}(OH)_2$	4.5
Amorphous	-	-

2.2. Chemical composition

XRF analysis (Table 2) showed that the sample zinc grade was 15.67%, with 0.42 % lead, which was negligible.

Table 2. Sample quantitative XRF analysis.

Element/Compound	SiO_2	BaO	CaO	Fe_2O_3	K_2O	MgO
Percentage	19.40	0.24	15.65	3.86	0.57	1.36
Element/Compound	MnO	SO_3	TiO_2	Pb	Zn	LOI
Percentage	0.14	0.41	0.20	0.42	15.67	24.67

2.3. Microscopic mineralogical studies

Microscopic studies were conducted on size-by-size polished sections with a fraction range of 1400 µm to 75 µm to determine the degree of liberation, which is calculated as the ratio of liberated particles to the sum of liberated and locked particles. According to the results presented in Table 3, a degree of liberation exceeding 80% for both smithsonite and hemimorphite occurs at sizes below 106 µm, as illustrated in Fig. 1.

Table 3. Microscopic Degree of liberation study.

Fraction (µm)	1400	600	212	150	106	75
Degree of liberation of smithsonite (%)	65-70	70-75	75-80	85-90	90-95	95
Degree of liberation of hemimorphite (%)	50-60	60-65	70-75	75-80	85-90	95

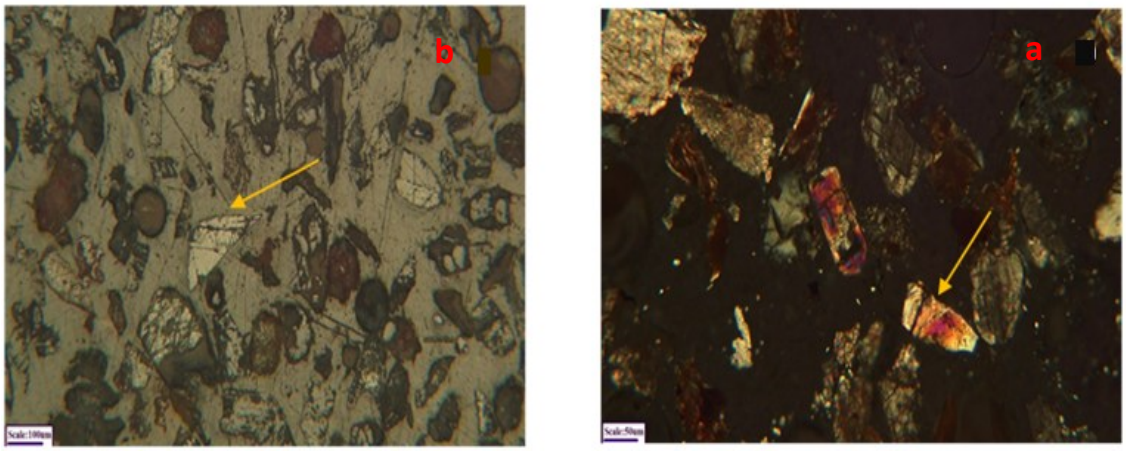

Fig. 1. Microscopic images of the 106 µm fraction. a) liberated hemimorphite particles, b) liberated lsmithsonite particles.

3. Materials and methods

The samples were initially crushed to below 3.36 mm in a closed circuit using primary and secondary jaw crushers with a control screen. Finally, the material remaining on the screen was fed into a roll crusher in a closed circuit with a control screen to obtain the final product with a size below 3.36 mm. The resulting product was homogenized using a riffle splitter, and ultimately, it was divided into 1-kilogram representative samples for further analysis and experiments.

To determine the optimal grinding time for the wet rod mill to achieve the desired degree of liberation (above 80%), the grinding of the mill feed with a weight of 1000 g, 50% solids, and a grinding load of 3539 g was conducted at times of 4, 5:30, 7, 8:30, and 10 minutes, with the results presented in Table 4. Based on the degree of liberation results, grinding times of 7 and 8:30 minutes were selected. The desliming test (using a 25-micrometer sieve and wet method) of the ground product at 7 and 8:30 minutes showed that 23.65% and 40.3% of the zinc metal, respectively, reported to the slimes.

Table 4. Grinding time and d80 of the ground product.

Grinding time (min)	4	5:30	7	8:30	10
d_{80} (µm)	150	110	92	75	69
Weight of -25 µm (gr)	196	224	285	331	412

The chemicals used in the flotation experiments are listed in Table 5 [19]. In all experiments, the following parameters were kept constant: pulp pH of 11, sodium silicate (500 g/t), sodium hexametaphosphate (250 g/t), pine oil (120 g/t), pulp solid percentage (14.8%), rotor speed (1000 rpm), feed weight, and cell volume. Scraping was conducted for 10 minutes in all tests, with intervals of 15 seconds. It is worth mentioning that the flotation experiments in this study were conducted without prior desliming of the feed.

Table 5. The chemicals used in flotation experiments.

Surfactant	**Concentration (%)**	**Role**	**Conditioning time (min)**
Sodium silicate	97	Depressant/Dispersant	5
Sodium hexametaphosphate	96	Depressant	5
Sodium sulfide	75	Sulfidant	10
Sodium hydroxide	-	pH regulator	Simultaneously with sodium sulfide
Acetate of coco amine (Armac C)	99	Collector	10
Pine oil	99	Frother	2

In this study, a two-phase vortex pump was used to generate nano-microbubbles, and its various parameters are presented in Table 6. To characterize these nano-microbubbles, Dynamic Light Scattering (DLS) was employed, specifically using a Brookhaven 90Plus model. This method, crucial for fine bubble characterization, relies on the principle of light scattering rather than direct imaging. A He-Ne laser (emitting at a wavelength of 632.8 nm) was used as the light source, directing its beam through the sample in a polystyrene or quartz cuvette. A detector, typically at a 90-degree angle, captured the light scattered by

the moving bubbles. Measurements were performed at a controlled 25 °C. DLS operates by analyzing fluctuations in scattered light intensity, which are caused by the Brownian motion of the bubbles; smaller bubbles move faster, causing more rapid fluctuations. The collected data were processed by dedicated particle sizing software to determine the hydrodynamic diameter of the bubbles. The accuracy of these measurements depends on precise input of parameters like the solvent's viscosity and refractive index. The DLS system used has an effective detection range of approximately 2 nm to 6 µm, suitable for nano-microbubbles. According to Fig. 2, the nano-microbubbles produced by this pump have a size distribution ranging between 100 and 500 nm, with a mean diameter of 300 nm and zeta potential of approximately -10 mV, which were utilized in the flotation experiments.

Table 6. Conditions for generating nano-microbubbles.

Frother concentration in the pump tank (g/t)	Frother addition time (min)	Circulation time of the solution in the pump (min)	Input air flow rate of the pump (L/min)	Input pressure difference of the pump (mmHg)	Output pressure difference of the pump (bar)	Average size of nano bubbles (nm)
10	0	10	2	180	2.6	300

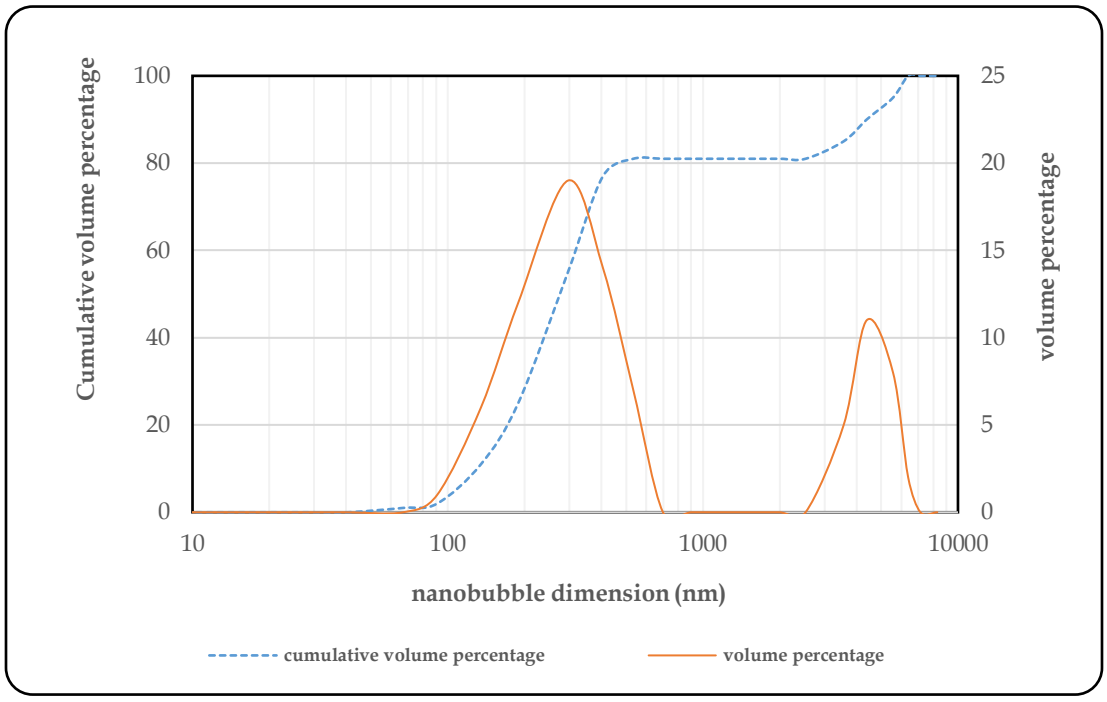

Fig. 2. Size distribution diagram of the nano-microbubbles generated under the mentioned conditions determined by DLS.

4. Results and Discussion

In this research, to investigate the effect of the presence and absence of nano-microbubbles on the flotation process, parameters such as feed particle size, sodium sulfide concentration, and Armac C concentration were evaluated. The experiments were conducted using DX11 design expert software and a two-level full factorial design method. The matrix of various conditions of the experiments related to this design, as well as the results, are presented in Table 7.

Table 7. The proposed experiments by the DX11 software using a two-level full factorial design method.

Test No.	Particle size (µm)	Armac C concentration (g/t)	Sodium sulfide concentration (g/t)	using nano-micro bubbles in water (%)	Concentrate grade (%)	Concentrate recovery (%)
1	92	1000	4000	100	25.89	88.81
2	92	1000	4000	0	27.31	81.74
3	92	1000	3000	0	17.08	30.52
4	75	800	4000	0	24.13	58.52
5	92	1000	3000	100	15.18	33.42
6	83	900	3500	50	19.20	50.24
7	92	800	4000	100	24.41	69.86
8	75	1000	3000	0	14.87	25.62
9	75	800	4000	100	22.99	62.35
10	75	1000	4000	100	23.97	68.07
11	83	900	3500	50	18.61	52.20
12	83	900	3500	50	19.83	48.10
13	83	900	3500	50	18.56	55.20
14	92	800	3000	100	13.73	27.16
15	92	800	4000	0	25.88	66.06
16	75	1000	4000	0	25.20	65.13
17	75	800	3000	100	12.42	23.38
18	92	800	3000	0	14.39	25.71
19	75	800	3000	0	13.61	22.15
20	75	1000	3000	100	13.48	27.96

ANOVA analysis was used to evaluate the results of the experiments, to determine the factors and interaction effects on the grade, recovery, and the validity of the model proposed by the software. The results are presented in Table 8. The findings indicate that the proposed model is valid, and the parameters influencing the model include the use of nano-microbubbles water (A), sodium sulfide concentration (B), Armac C concentration (C), particle size (D), as well as the interactions BC, BD, CD, and BCD. In addition, the statistical analysis of the model evaluation shows that the model has sufficient accuracy.

Table 8. ANOVA analysis.

Source	Sum of squares	df	Mean square	F value	P value Prob>F	
Model	8230.55	8	1028.82	171.14	<0.0001	Significant
A- using nano-microbubble water	40.83	1	40.83	79.6	<0.0244	
B- Sodium sulfide concentration	7422.68	1	7422.68	1234.76	<0.0001	
C- Armac C concentration	272.91	1	272.91	45.40	<0.0001	
D- Particle size	307.13	1	307.13	51.09	<0.0001	
BC	48.44	1	48.44	8.06	0.0161	
BD	75.26	1	75.26	12.52	0.0046	
CD	40.07	1	40.07	6.67	0.0255	
BCD	23.23	1	23.23	3.86	0.0751	
Residual	66.13	11	6.01			
Lack of fit	38.82	8	4.85	0.5330	0.7880	Not significant
Pure error	27.31	3	9.10			
Cor Total	8296.68	19				
R^2= 0.9920	Standard deviation= 2.45			Adjusted R^2= 0.9862		
Predicated R^2= 0.9832	Adequate precision= 39.9487					

Based on the results presented in Fig. 3, it is evident that the presence of nano-microbubbles (A) has led to an enhancement in zinc recovery. This improvement can be attributed to the unique characteristics of nano-microbubbles. Their significantly small size provides a considerable specific surface area, resulting in a substantial increase in the number of bubbles per unit volume of the flotation cell. Consequently, this notably improves the probability of effective collision between fine and ultrafine zinc oxide particles and the bubbles. Furthermore, at the nano scale, the larger contact area and stronger capillary forces can establish a more robust attachment between particles coated with a nanobubble film and larger bubbles. This more stable attachment reduces the probability of coarse particle detachment from the bubbles under the influence of shear forces within the flotation cell, ultimately improving the recovery. Additionally, the slower ascent velocity of nano-microbubbles compared to conventional bubbles may increase the residence time of the bubbles, providing more opportunity for hydrophobic particles to adhere to the bubble surfaces. Finally, the bursting of nano-microbubbles in the vicinity of particle surfaces can lead to the generation of localized micro turbulences, which facilitate a more effective transfer of particles to the froth phase. As the results demonstrate, increasing the share of nano-microbubble water from 0 to 100% while keeping other parameters constant (at their midpoint) led to an increase in zinc recovery from 47.51% to 50.71%. Among the investigated parameters, the concentration of sodium sulfide (B) had the most significant impact on zinc recovery in the concentrate. When its concentration increased from 3000 g/t to 4000 g/t (with other parameters held constant), the zinc recovery increased from 27.57% to 70.65%. This improvement can be attributed to the reaction of sulfide ions (S_2^-) present in the solution with the surface of oxide minerals,

leading to the formation of a metal sulfide layer (such as ZnS) on their surface. This surface sulfidation, by creating more active sites, facilitates collector adsorption and consequently results in the formation of a stronger hydrophobic layer on the particles, increasing their tendency to attach to air bubbles. The high concentration of sodium sulfide is likely attributed to two factors: its role as a pH regulator (hydrolysis of sodium sulfide yields hydroxide ions, resulting in an elevation of the solution's pH) and the potential increase in sodium sulfide consumption due to the presence of slimes. Additionally, increasing the concentration of Armac C collector (C) from 800 g/t to 1000 g/t (with other parameters held constant) resulted in an 8.26% increase in recovery, with zinc recovery rising from 44.98% to 53.24%. This improvement is likely due to increased surface hydrophobicity caused by the higher collector concentration and the increased contact angle at higher concentrations, which enhances particle-bubble attachment. Furthermore, increasing the feed particle size (D) leads to better flotation performance because fewer fines are generated during grinding. For instance, when the feed particle size was increased from -75 μm to -92 μm, the zinc recovery increased from 44.73% to 53.49%.

As indicated, the interactions of parameters BC, BD, CD, and BCD had a significant effect on the response, and their contour and three-dimensional plots are presented in Fig. 4. The interactions of all parameters on the response were positive, increasing recovery.

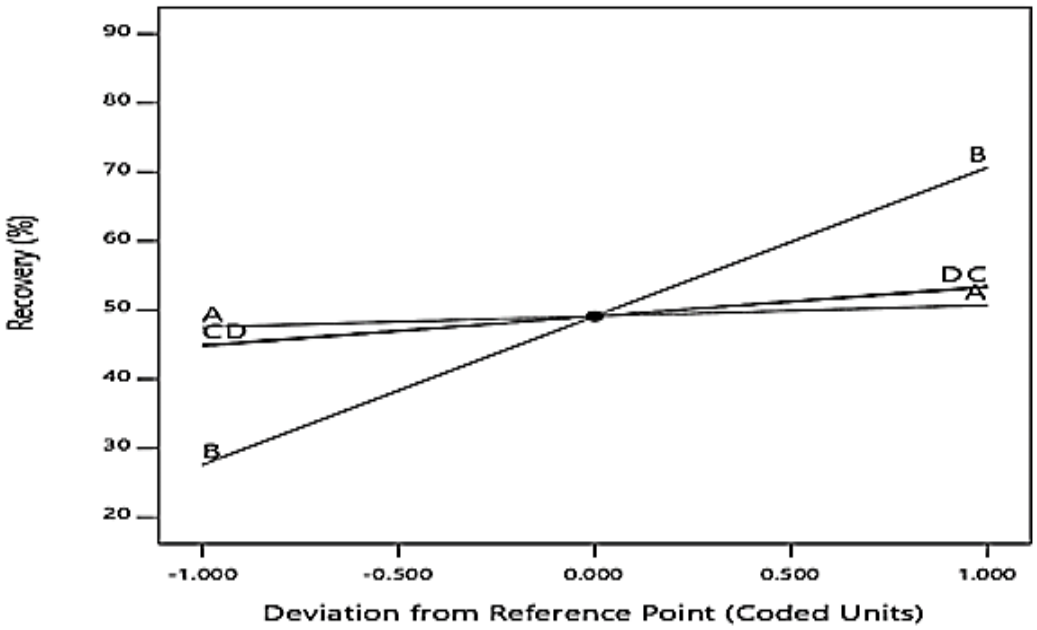

Fig. 3. Perturbation plot.

Based on the response surface equation, the optimization of effective parameters to achieve the maximum zinc recovery in the concentrate is shown in Fig. 5. According to these results, the maximum zinc recovery was achieved when the nano-microbubbles water was 100%, the sodium sulfide concentration was 4000 g/t, the Armac C concentration was 1000 g/t, and the d80 of the feed particles was 92 μm. Under these conditions, a concentrate with a grade of 25.74% and a recovery of 87.45% was obtained. Compared to the absence of nano-microbubbles, this represents an approximate 7% increase in zinc recovery.

a)

b)

c)

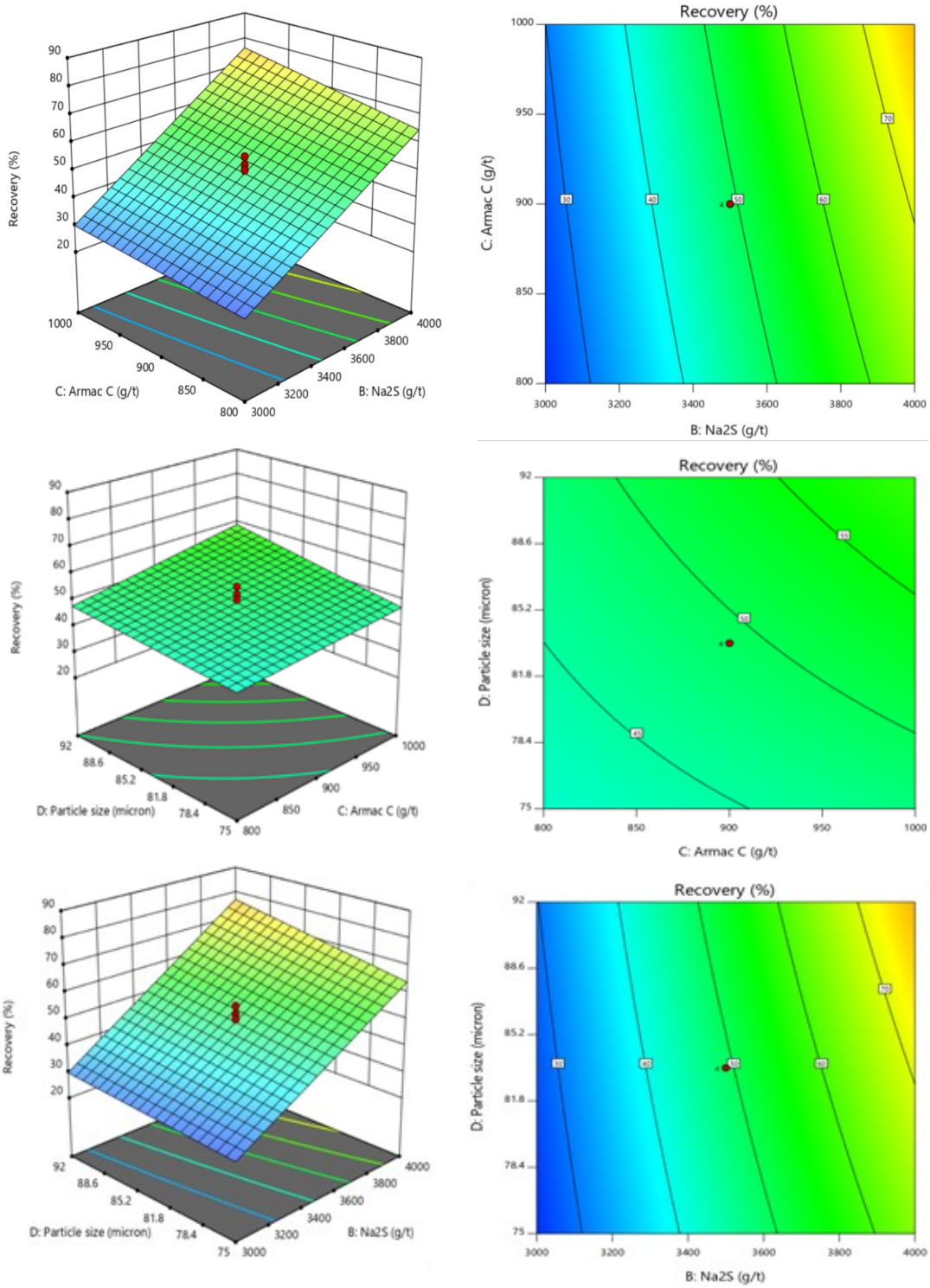

Fig. 4. Contour and three-dimensional plots showing the interaction effects of: a) BC, b) BD, c) CD, on recovery.

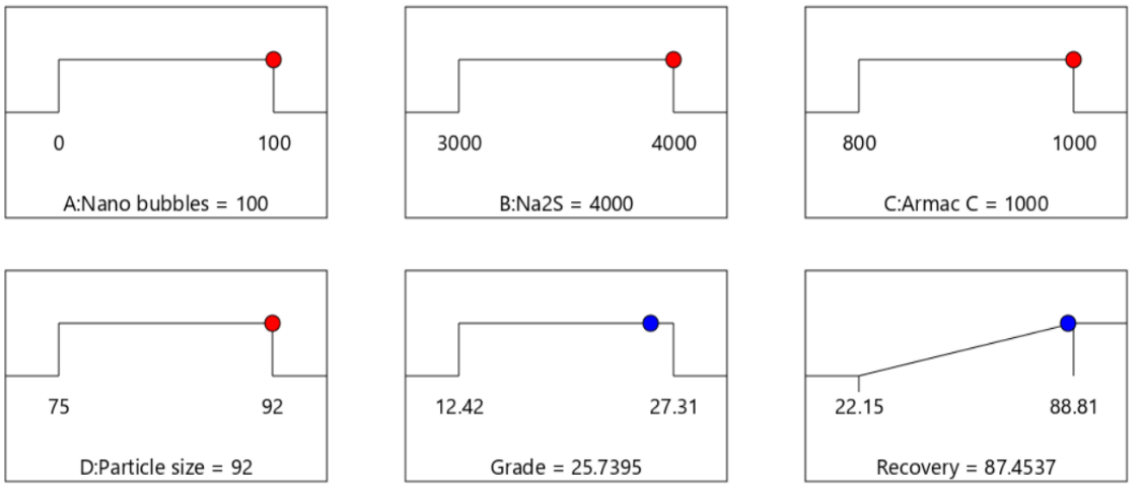

Fig. 5. Optimization results to achieve maximum zinc recovery.

Given the role of nano-microbubbles as a promoter, a comparison was made between the impact of using nano-microbubbles and potassium amyl xanthate (PAX) as a promoter under optimized conditions. The results are presented in Table 9. The application of PAX at 100 g/t and 200 g/t concentrations resulted in a marginal recovery increase of 0.35% and 0.84%, respectively, which was significantly lower than the 7.07% improvement observed when nano-microbubbles were used. The superior performance of nano-microbubbles as a promoter in enhancing zinc recovery is likely attributed to their ability to establish a more efficient and uniform hydrophobic coating on the particle surface. In contrast, the effectiveness of PAX in inducing hydrophobicity relies on its chemical or physical adsorption at the active sites of the mineral surface.

Table 9. Comparison of the effect of PAX with nano-microbubbles under optimized conditions.

Test No.	using nano-microbubbles water (%)	PAX (g/t)	Concentrate grade (%)	Concentrate recovery (%)
1	0	0	27.31	81.74
2	0	100	26.02	82.09
3	0	200	25.92	82.58
4	0	300	24.21	77.20
5	100	0	25.89	88.81

5. Conclusions

In contrast to previous studies, this research aimed to investigate the effect of the presence and absence of nano-micro bubbles in the flotation process of zinc oxide minerals without feed desliming. The sample was provided by the Iranian Lead and Zinc Plant located in Zanjan Province, and it contains valuable minerals such as smithsonite and hemimorphite. Four parameters were examined: the use of nano-microbubble water, sodium sulfide concentration, Armac C concentration, and feed particle size. By examining the use of nano-microbubble water from 0% to 100% while keeping other factors at their midpoint values, it was found that zinc recovery increased from 47.51% to 50.71%. This 3.2% increase may be attributed to the higher probability of fine particle collisions and the enhanced probability of coarse

particles attaching to conventional bubbles. When evaluating sodium sulfide concentrations of 3000, 3500, and 4000 g/t, it was determined that this parameter had the most significant impact on flotation among the studied parameters. Increasing the sodium sulfide concentration from 3000 g/t to 4000 g/t resulted in a 43.08% increase in zinc recovery, rising from 27.57% to 70.65%. This improvement could be attributed to enhanced sulfidation of the zinc oxide mineral surfaces, which improves collector adsorption on the particle surfaces. To investigate the effect of Armac C concentration on flotation, concentrations of 800, 900, and 1000 g/t were examined. The results showed that increasing the Armac C concentration from 800 to 1000 g/t (while keeping other parameters at their midpoint values) increased zinc recovery from 44.98% to 53.24%. This improvement was likely due to an increase in the particle-bubble contact angle. Additionally, it was found that reducing the particle size, d80, from 92 μm to 75 μm led to a decrease in zinc recovery from 53.49% to 44.73%. This was because the rod mill grinding product contained more slimes, which may increase chemical consumption and reduce recovery. Finally, by optimizing the studied parameters, it was concluded that maximum zinc recovery was achieved when the use of nano-microbubble water was 100%, the sodium sulfide concentration was 4000 g/t, the Armac C concentration was 1000 g/t, and the d80 of the feed particles was 92 μm. Under these conditions, a concentrate with a grade of 25.89% and a recovery of 88.81% was obtained, representing an approximately 7% increase in zinc recovery compared to the absence of nano-microbubbles. Furthermore, the results indicated that the application of potassium amyl xanthate as a promoter, compared to the presence of nano-microbubbles, resulted in a lower recovery increase, approximately 1% at a PAX concentration of 200 g/t. In conditions where neither nano-microbubbles nor PAX were used, the concentrate grade and recovery were 27.31% and 81.74% respectively.

Ethical Considerations

The authors avoided data fabrication, falsification, and plagiarism, and any form of misconduct.

Funding

This research did not receive any specific grant from funding agencies in the public, commercial, or not-for-profit sectors.

Conflict of Interest

The authors declare no conflict of interest.

References

[1] Farrokhpay, M., Irannajad, M., & Gharabaghi, M. (2021). Flotation of fine particles: A review, *Mineral Processing and Extractive Metallurgy Review,* 42 (7): 473-483. https://doi.org/10.1080/08827508.2020.1793140

[2] Trahar, w., Warren, L. (1976). The flotability of very fine particles-A review. *International Journal of Mineral Processing,* 3(2): 103-131. https://doi.org/10.1016/0301-7516(76)90029-6

[3] Rezai, B. (2017). Nanobubbles effect on the mechanical flotation of phosphate ore fine particles. *Physicochemical Problems of Mineral Processing*. https://doi.org/10.5277/ppmp1804

[4] Ma, F., Zhang, P., & Tao, D. (2022). Surface nanobubble characterization and its enhancement mechanisms for fine-particle flotation: A review. *International Journal of Minerals, Metallurgy and Materials*, 29(4): 727-738. https://doi.org/10.1007/s12613-022-2450-3

[5] Maoming, Fan, Tao, D., Honaker, R., Luo, Z. (2010). Nanobubble generation and its applications in froth flotation (part II): fundamental study and theoretical analysis. *Mining Science and Technology (China),* 20 (2): 159-177. https://doi.org/10.1016/S1674-5264(09)60179-4

[6] Hampton, M. A., Nguyen, A. V. (2010). Nanobubbles and the nanobubble bridging capillary force. *Advances in colloid and interface science,* 154 (1-2): 30-55. https://doi.org/10.1016/j.cis.2010.01.006
[7] Tao, D. (2005). Role of bubble size in flotation of coarse and fine particles-a review. *Separation science and technology,* 39 (4)*:* 741-760. https://doi.org/10.1081/SS-120028444
[8] Nazari, S., Zhou, S., Hassanzadeh, A., Li, J., Bu, X., & Kowalczuk, P. B. (2022). Influence of operating parameters on nanobubbles -assisted flotation of graphite. *Journal of Materials Research and Technology,* 20: 3891-3904. https://doi.org/10.1016/j.jmrt.2022.08.137
[9] Sobhy, A., Tao, D. (2019). Effects of nanobubbles on froth stability in flotation column. *International Journal of Coal Preparation and Utilization,* 39 (4): 183-198. https://doi.org/10.1080/19392699.2018.1459582
[10] Nikouei Mahanni, N., Karamoozian, M., Jahani Chegeni, M., & Mahmoodi Meymand, M. (2024). Effect of stable nano-microbubbles on sulfide copper flotation and reduction of chemicals dosage. *Journal of Mining and Enviroment,* 15 (1): 261-283. https://doi.org/10.22044/jme.2023.13205.2413
[11] Rosa, A. F., & Rubio, J. (2018). On the role of nanobubbles in particle–bubble adhesion for the flotation of quartz and apatitic minerals. *Minerals Engineering*, 127: 178-184. https://doi.org/10.1016/j.mineng.2018.08.020
[12] Kyzas, G. Z., Mitropoulos, A. C., & Matis, K. A. (2021). From microbubbles to nanobubbles: effect on flotation. *Processes*, 9(8): 1287. https://doi.org/10.3390/pr9081287
[13] Nazari, S., Bu, X., Hassanzadeh, A., Li, J., Zhou, S., & Kowalczuk, P. B. (2022). Recent developments in generation, detection and application of nanobubbles in flotation. *Minerals*, 12 (4): 462. https://doi.org/10.3390/min12040462
[14] Wang, X., Yuan, S., Liu, J., Zhu, Y., & Han, Y. (2022). Nanobubble-enhanced flotation of ultrafine molybdenite and the associated mechanism. *Journal of Molecular Liquids*, 346: 118312. https://doi.org/10.1016/j.molliq.2021.118312
[15] Zinjenab, Z. T., Azimi, E., Shadman, M., Hosseini, M. R., Abbaszadeh, M., & Namgar, S. M. (2023). Nano-microbubbles and feed size interaction in lead and zinc sulfide minerals flotation. *Chemical Engineering and Processing-Process Intensification*, 189: 109401. https://doi.org/10.1016/j.cep.2023.109401
[16] Pourkarimi, Z., Rezai, B., & Noaparast, N. (2017). Effective parameters on generation of nanobubbles by cavitation method for froth flotation applications *Physicochemical Problems of Mineral Processing,* 53(2): 920-942. https://doi.org/10.5277/ppmp170220
[17] Holl, J. W. (1970). Nuclei and Cavitation. *The American Society of Mechanical Engineerings,* 681–688. https://doi.org/10.1115/1.3425105
[18] Meegoda, J. N., Aluthgun Hewage, S., & Batagoda, J. H. (2018). Stability of nanobubbles. *Environmental Engineering Science,* 35 (11):1216-1227. https://doi.org/10.1089/ees.2018.0203
[19] Ejtemaei, S., Filippov, L., & Farnasiero, D. (2011). Influence of important factors on flotation of zinc oxide mineral using cationic, anionic and mixed (cationic/anionic) collectors, *Minerals Engineering,* 24 (13): 1402-1408. https://doi.org/10.1016/j.mineng.2011.05.018